Design of adaptive supramolecular polymer networks for healthcare materials

Dr. H. Kim[1], Dr. S. Park[1], Dr. J. Lee[1], Dr. D. Jung[1]*

[1] Department of Clinical Medicine and Biomedical Sciences, Hanyang University College of Medicine, Seoul, South Korea

Table of contents

1. NMR spectra

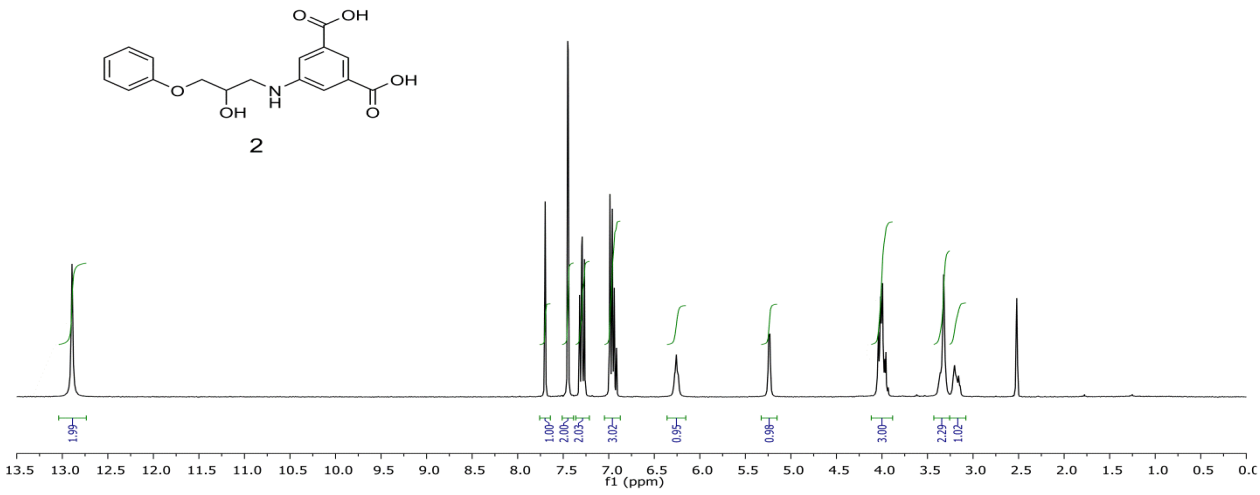

Figure S1. ^{1}H NMR spectrum (DMSO-d6) of the primary aminolysis product **2** obtained in the model reaction between phenyl glycidyl ether and 5-aminoisophthalic acid.

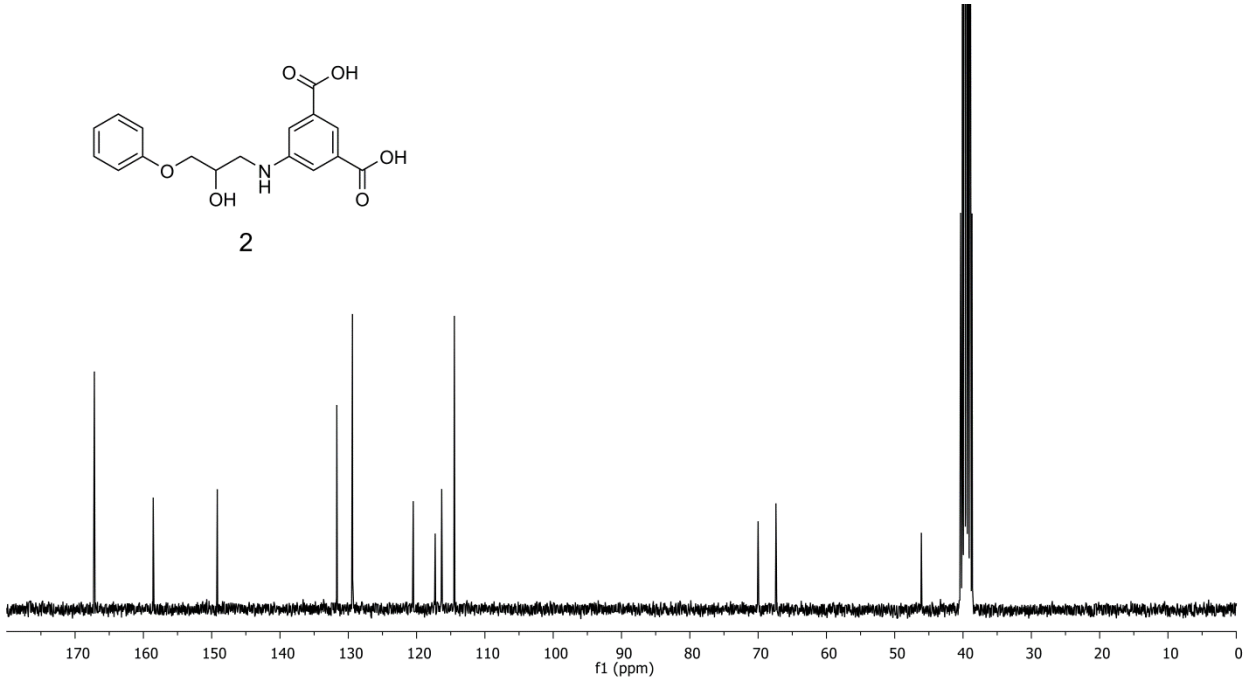

Figure S2. ^{13}C NMR spectrum (DMSO-d6) of the primary aminolysis product **2** obtained in the model reaction between phenyl glycidyl ether and 5-aminoisophthalic acid.

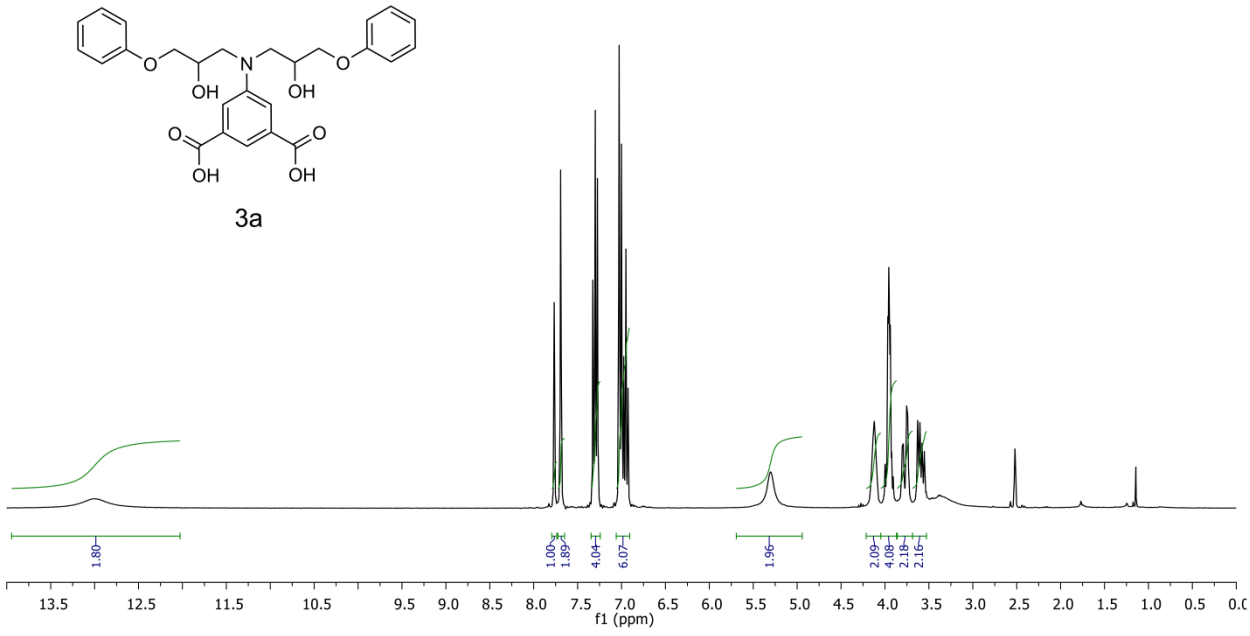

Figure S3. [1]H NMR spectrum (DMSO-d6) of the secondary aminolysis product **3a** (first diastereomer isolated of **3**) obtained in the model reaction between phenyl glycidyl ether and 5-aminoisophthalic acid.

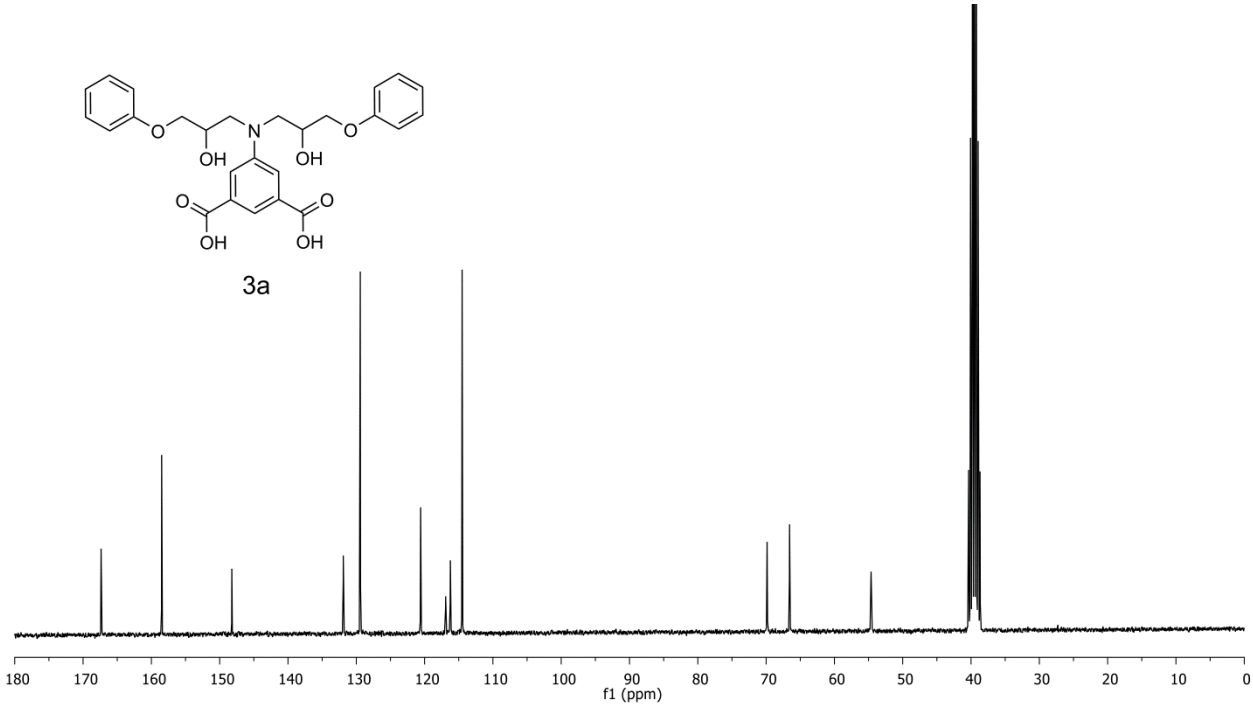

Figure S4. [13]C NMR spectrum (DMSO-d6) of the secondary aminolysis product **3a** (first diastereomer isolated of **3**) obtained in the model reaction between phenyl glycidyl ether and 5-aminoisophthalic acid.

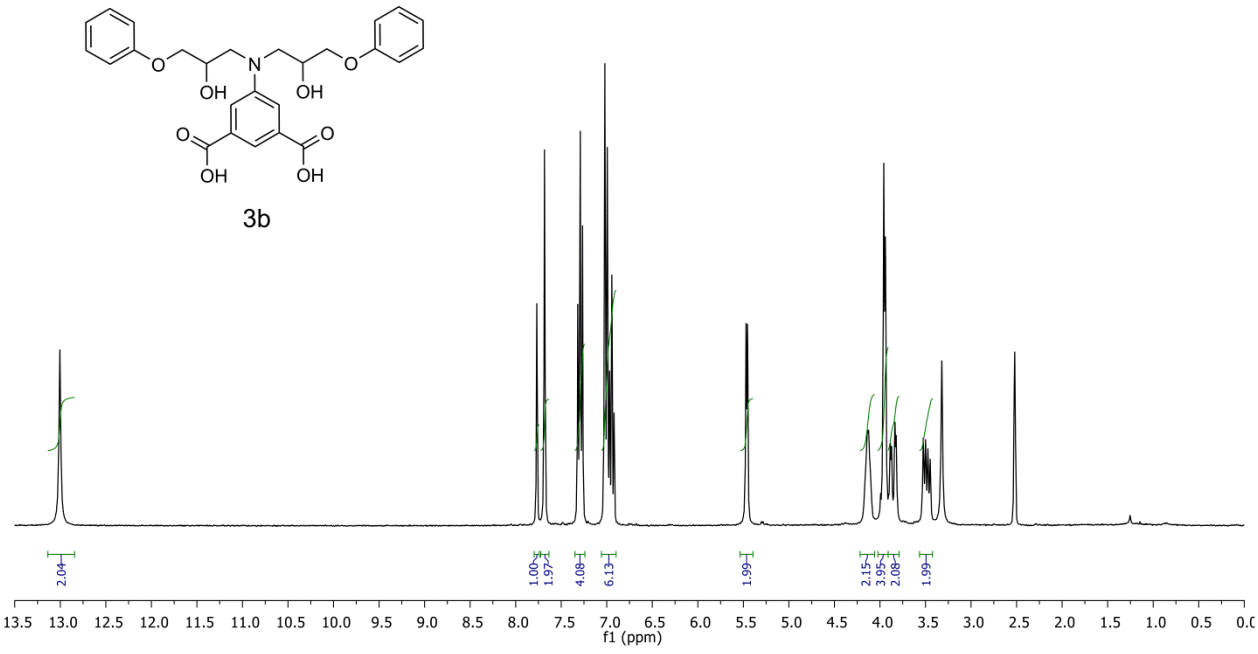

Figure S5. [1]H NMR spectrum (DMSO-d6) of the secondary aminolysis product **3b** (second diastereomer isolated of **3**) obtained in the model reaction between phenyl glycidyl ether and 5-aminoisophthalic acid.

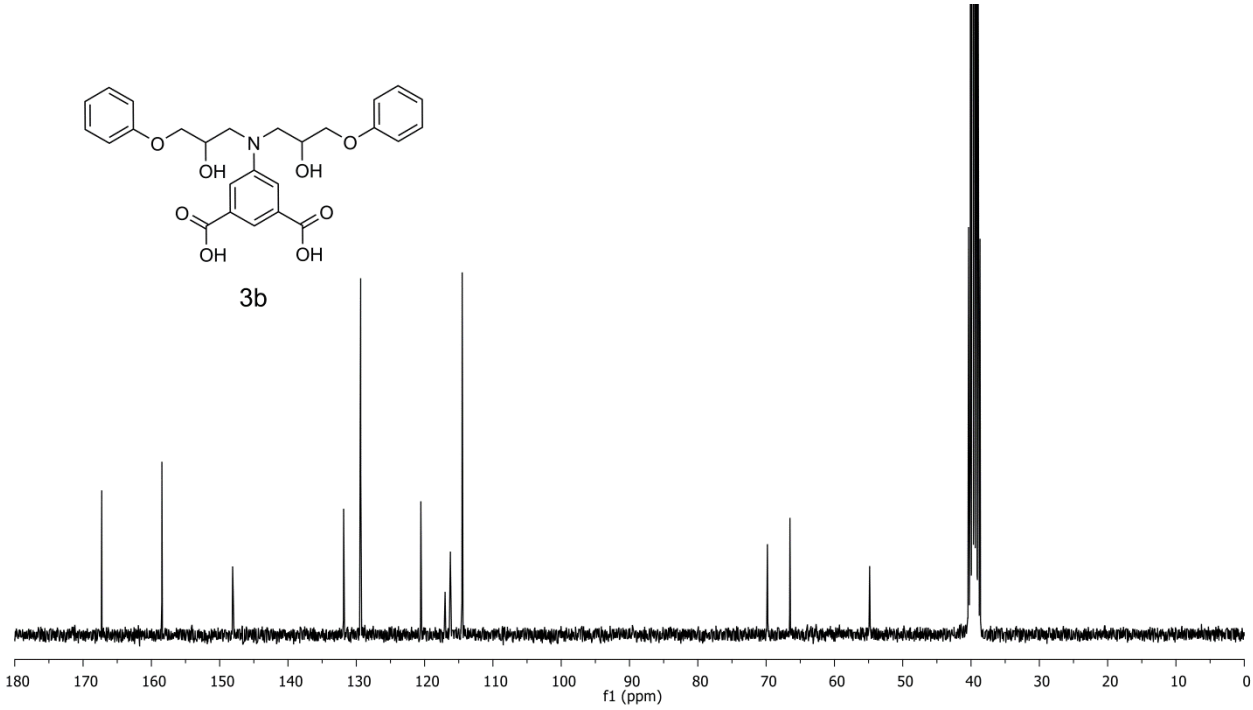

Figure S6. [13]C NMR spectrum (DMSO-d6) of the secondary aminolysis product **3b** (second diastereomer isolated of **3**) obtained in the model reaction between phenyl glycidyl ether and 5-aminoisophthalic acid.

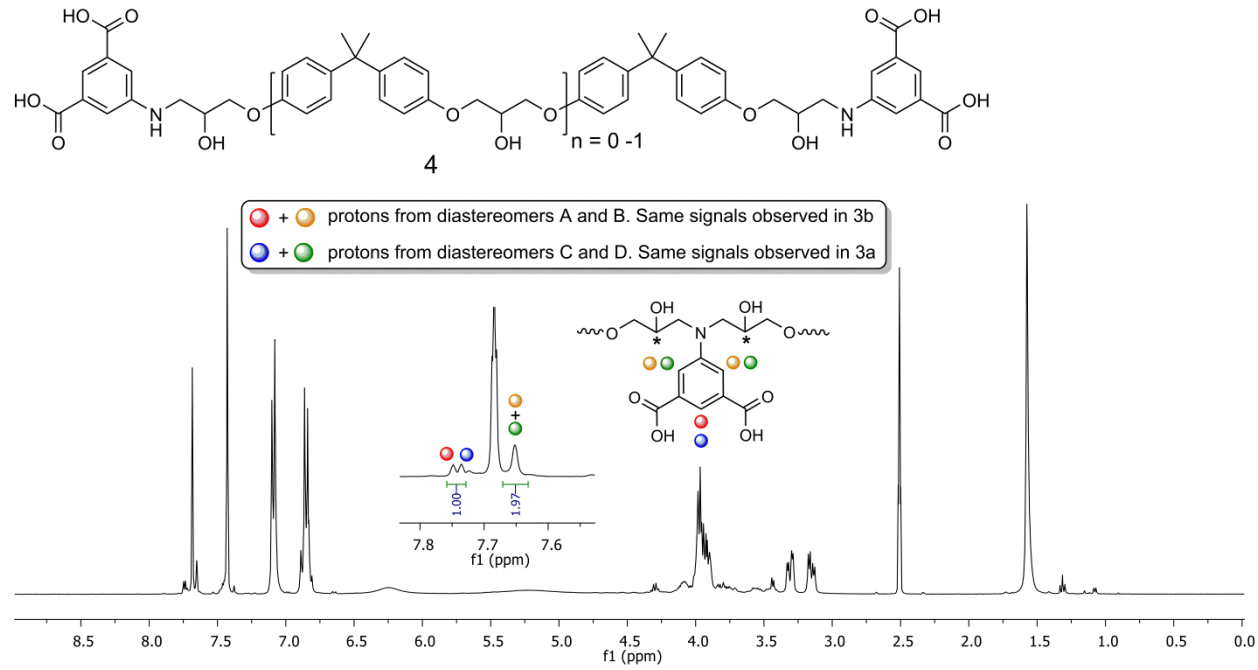

Figure S7. [1]H NMR spectrum (DMSO-d6) of IPA-functional mixture **M1**. The major signals belong to compound **4** (see experimental part for peaks assignment) and the highlighted minor signals belong to minor secondary aminolysis product **5** (only aromatic region is shown in detail for the shake of clarity, other minor

signals are the same as for diastereomers **3a** and **3b** in Figures S3 and S5 and are assigned in the experimental part), which introduce branching points. The IPA groups located at the branching points are also considered when calculating the stoichiometry of COOH/Py groups via ^{1}H NMR (see experimental part).

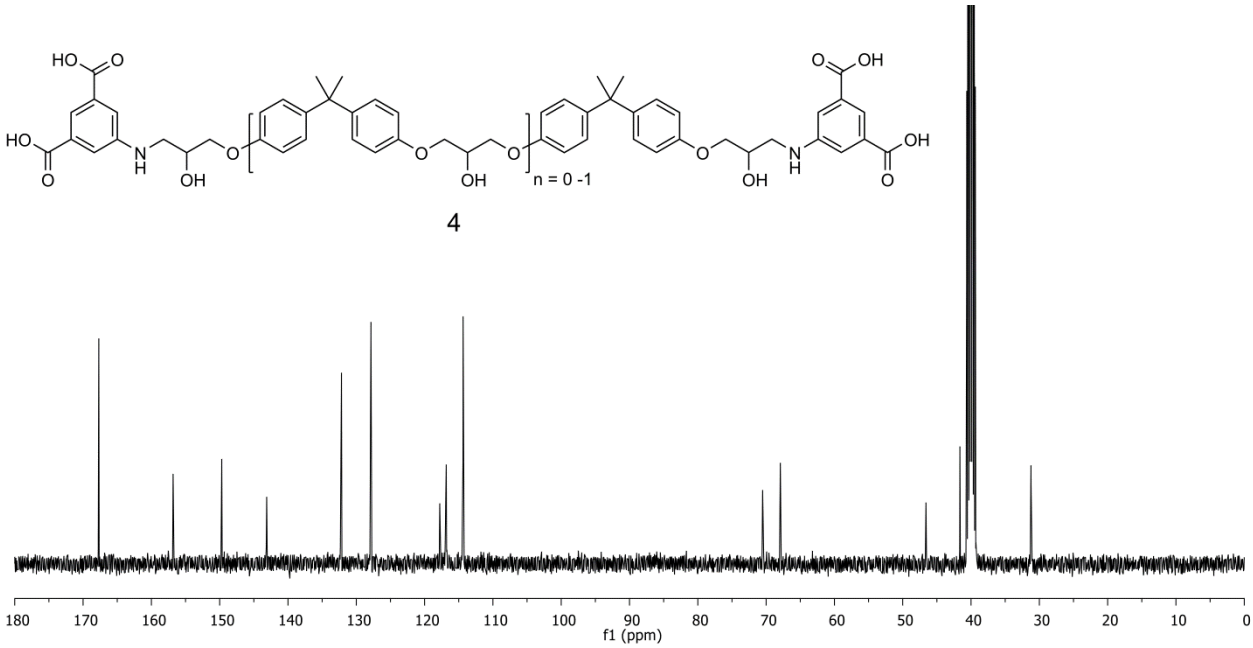

Figure S8. ^{13}C NMR spectrum (DMSO-d6) of M1 where the signals of IPA-functional compound **4** are observed.

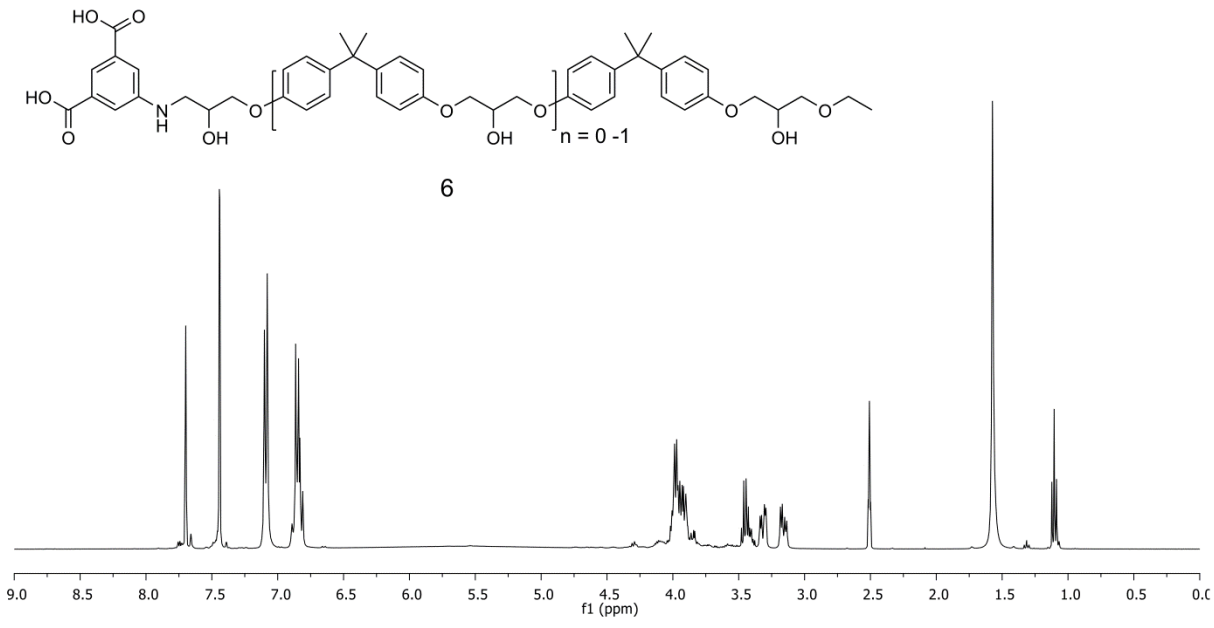

Figure S9. ^{1}H NMR spectrum (DMSO-d6) of IPA-functional mixture **M2**. The major signals belong to compound **6** (it is however not possible to differentiate here the signals of **6** from those of **4** or the bis(ethyloxy) derivative)). As for **M1** (see Figure S7), IPA branching points are observed as a result of minor secondary aminolysis giving compound **8** and must be considered when determining the stoichiometric ratio between

COOH/Py groups. The integration of the branching points shows that 7 mol% of amino-IPA groups undergo secondary aminolysis to produce branched compound **8**.

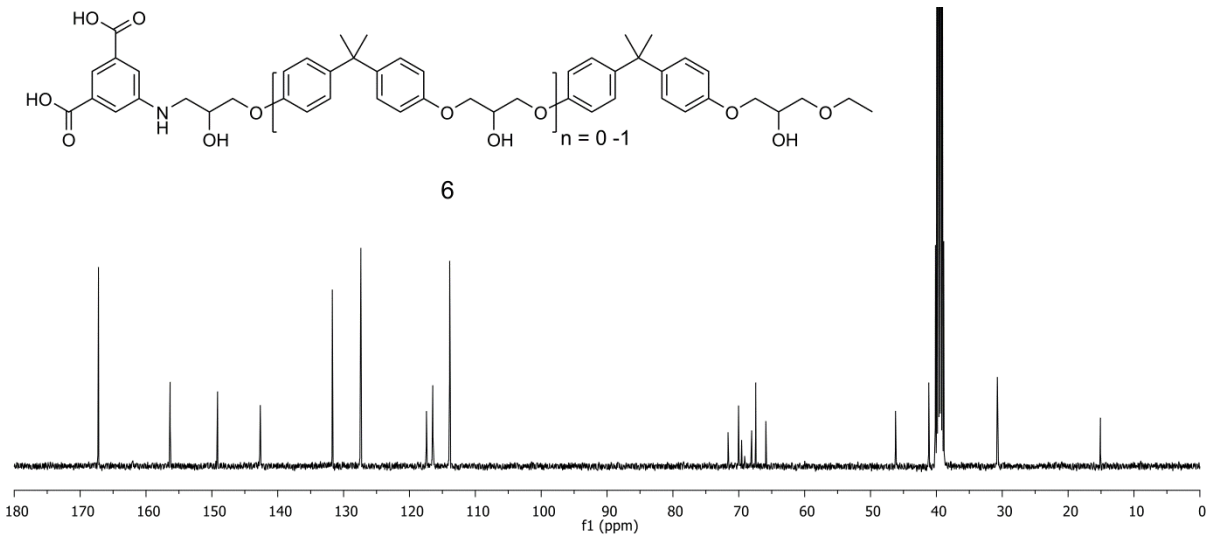

Figure S10. ^{13}C NMR spectrum (DMSO-d6) of **M2** where the signals of IPA-functional compound **6** (it is not possible to differentiate here the signals of **6** from those of **4** or the bis(ethyloxy) derivative) are observed.

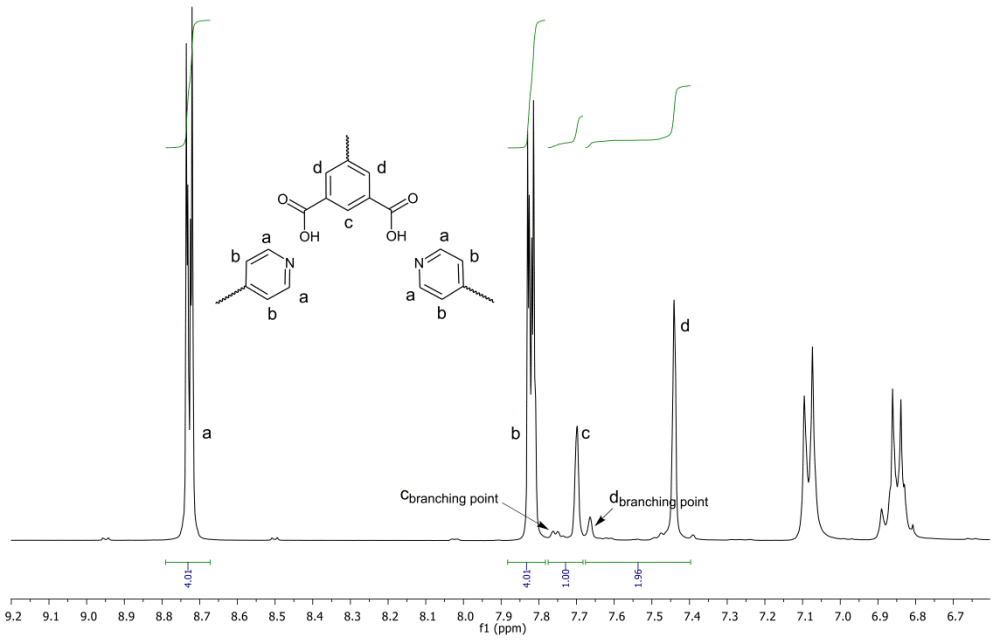

Figure S11. ^{1}H NMR spectrum (DMSO-d6) of **P1a** in which the integrals of the signals associated with the isophthalic acid group (**c** and **d**) and those associated with the pyridine groups (**a** and **b**) show the desired 1:1 ratio of COOH and pyridine groups.

2. Thermogravimetric analyses

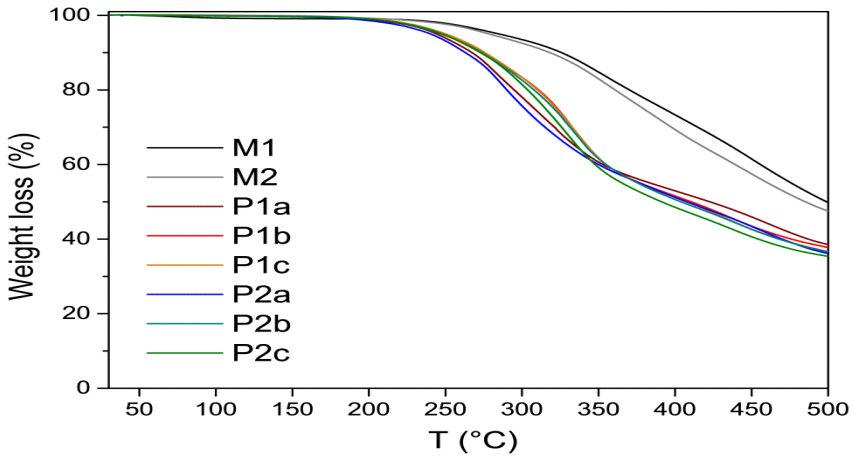

Figure S12. Thermogravimetric analyses of IPA-functional mixtures **M1** and **M2** and IPA-Py based supramolecular networks **P1a-c** and **P2a-c**.

3. FTIR spectra

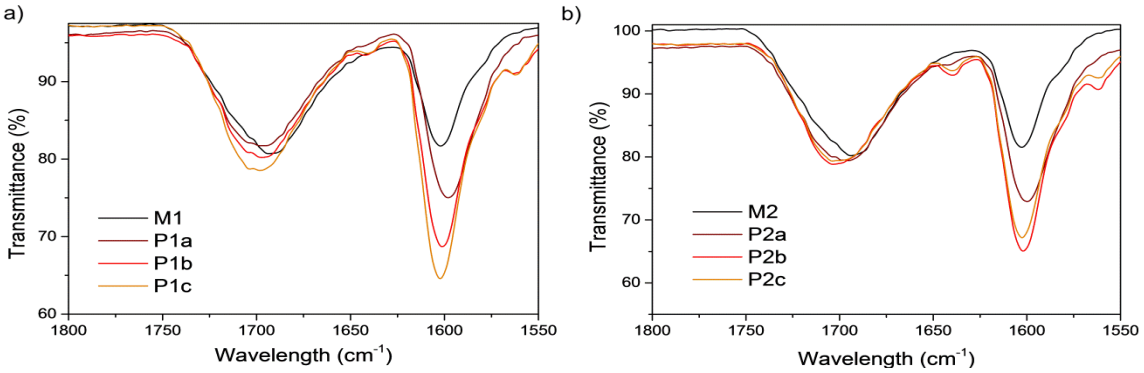

Figure S13. FTIR spectra (carbonyl region) of a) **M1** and supramolecular networks **P1a-c** and b) **M2** and supramolecular networks **P2a-c** evidencing the formation of a COOH-Py H-bonded network by the shift of the carbonyl stretching vibration from 1693 cm^{-1} to 1698 cm^{-1}.

4. Processing of supramolecular polymer fibers

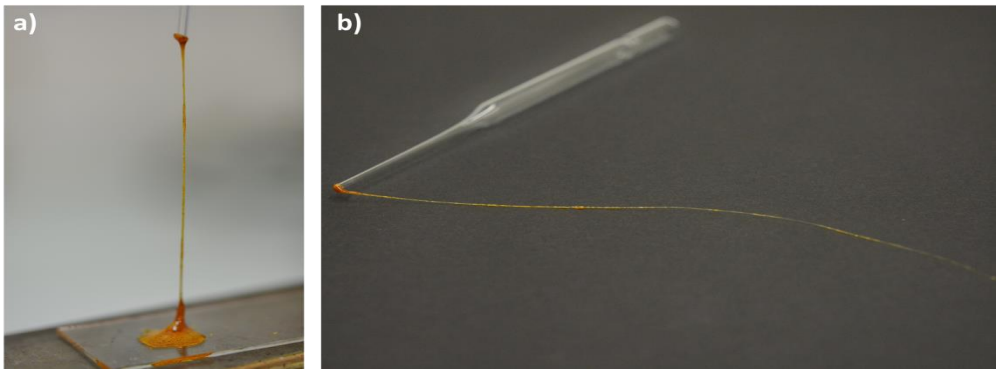

Figure S14. Pictures of fibers drawn from the melt of a) **M2** and b) **P1a**.

5. X-ray scattering

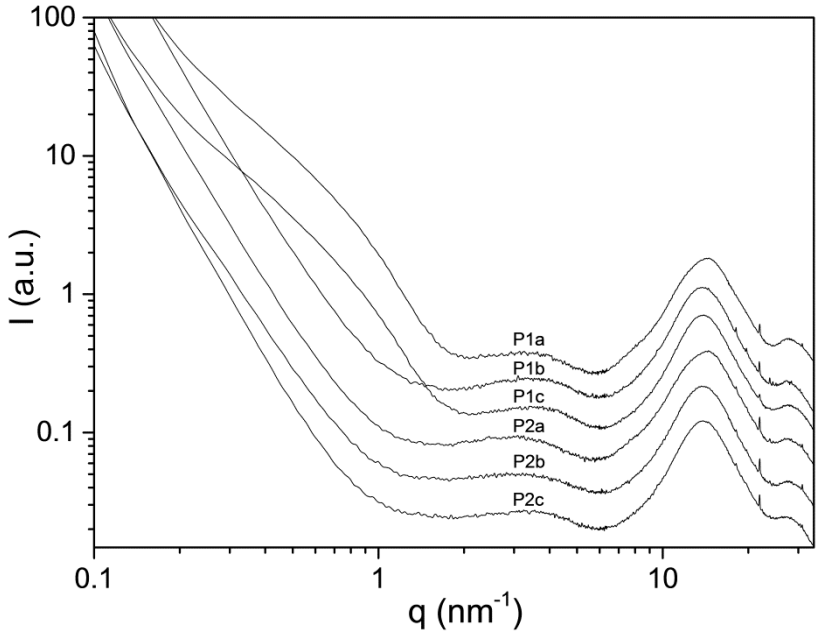

Figure S15. Combined SAXS/WAXS spectra of supramolecular networks **P1a-c** and **P2a-c** after annealing for 4 months in a desiccator at room temperature.

6. Differential scanning calorimetry

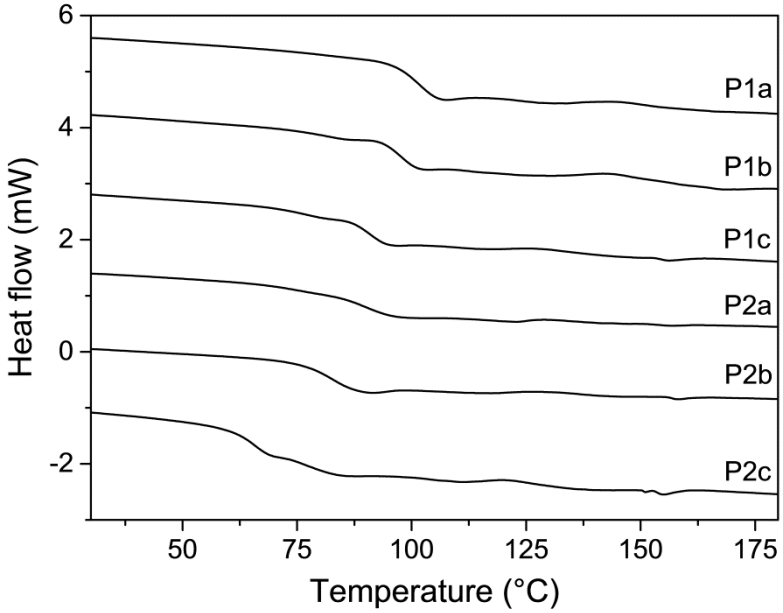

Figure S16. DSC traces of supramolecular networks **P1a-c** and **P2a-c** after annealing for 4 months in a desiccator at room temperature.

7. Rheology

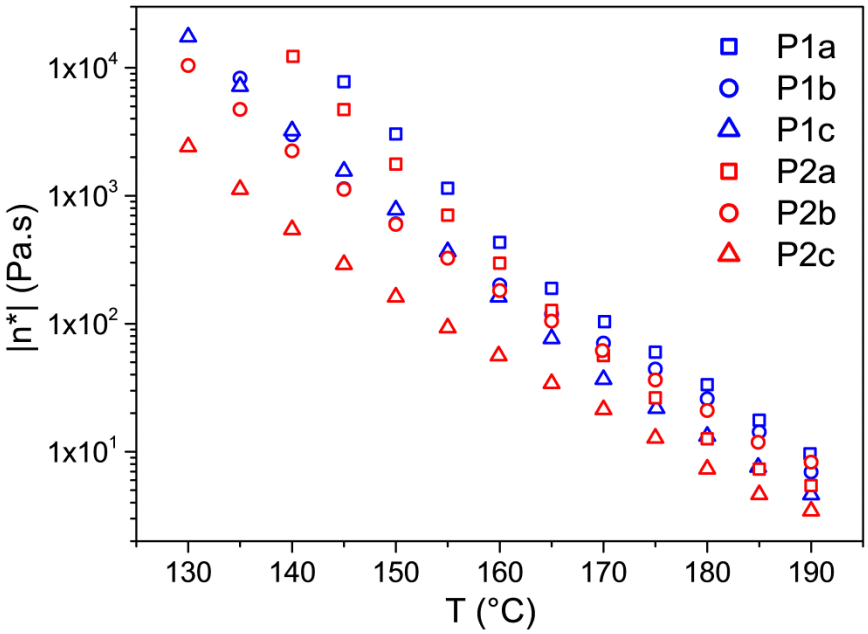

Figure S17. Complex viscosity of supramolecular networks **P4a-c** and **P5a-c** as a function of temperature. Data recorded at 20 rad/s.

Table S1. Melt viscosity of **P4a-c**, **P5a-c** at 190 °C measured by rheology at 100 rad/s.

Polymer	**|η*| (190 °C) (Pa·s)**
P1a	6.88
P1b	4.99
P1c	2.85
P2a	3.77
P2b	5.23
P2c	2.09

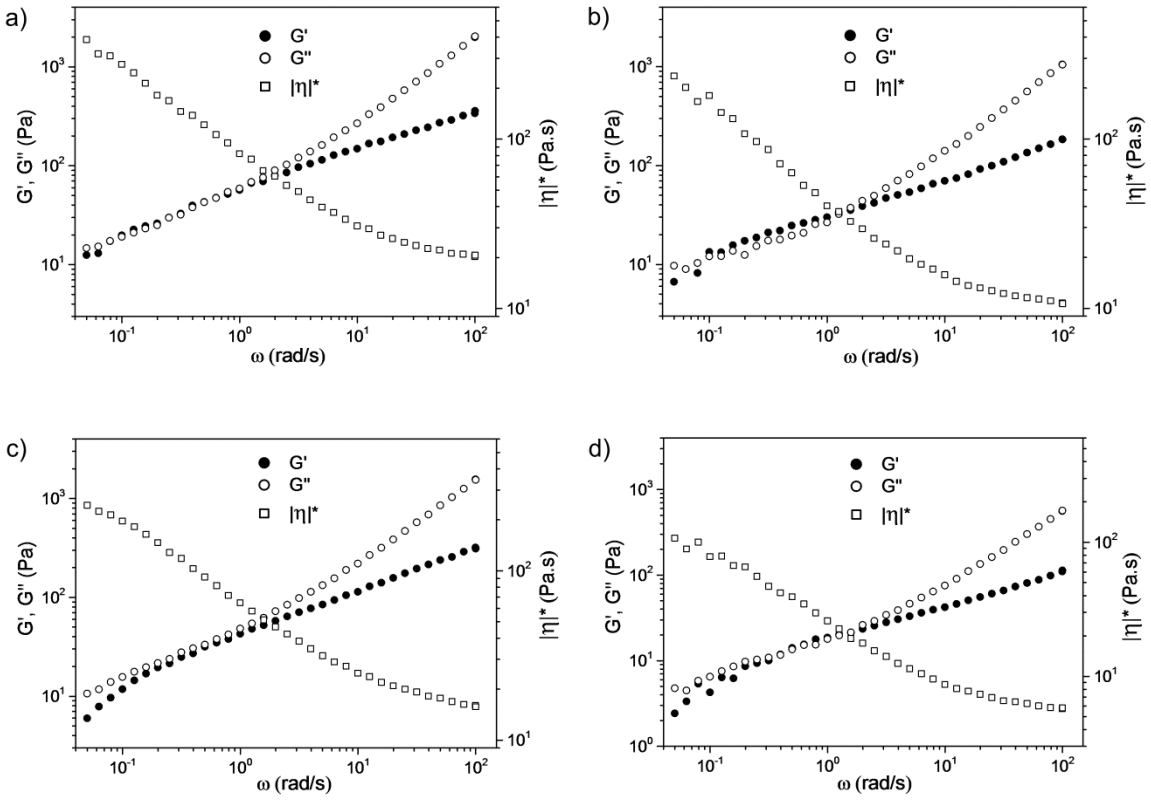

Figure S18. Frequency dependence of the elastic (●) and viscous (○) moduli and the complex viscosity (□) of a) **P1b**, b) **P1c**, c) **P2b** and d) **P2c** at 180 °C.

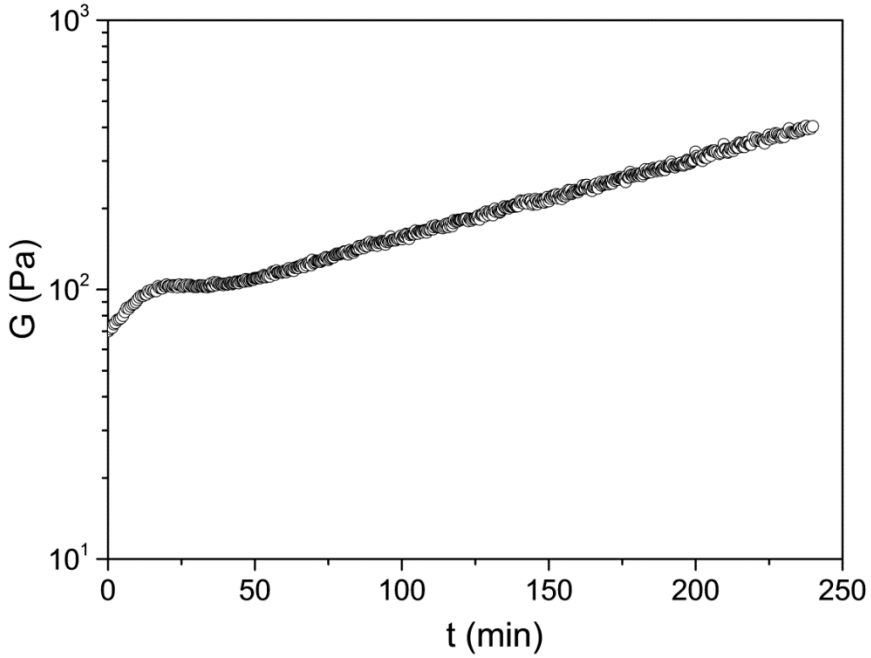

Figure S19. Shear modulus of supramolecular network **P1b** as a function of time at a constant temperature of 180 °C and 6.28 rad/s.

8. ^{1}H NMR study of thermal degradation

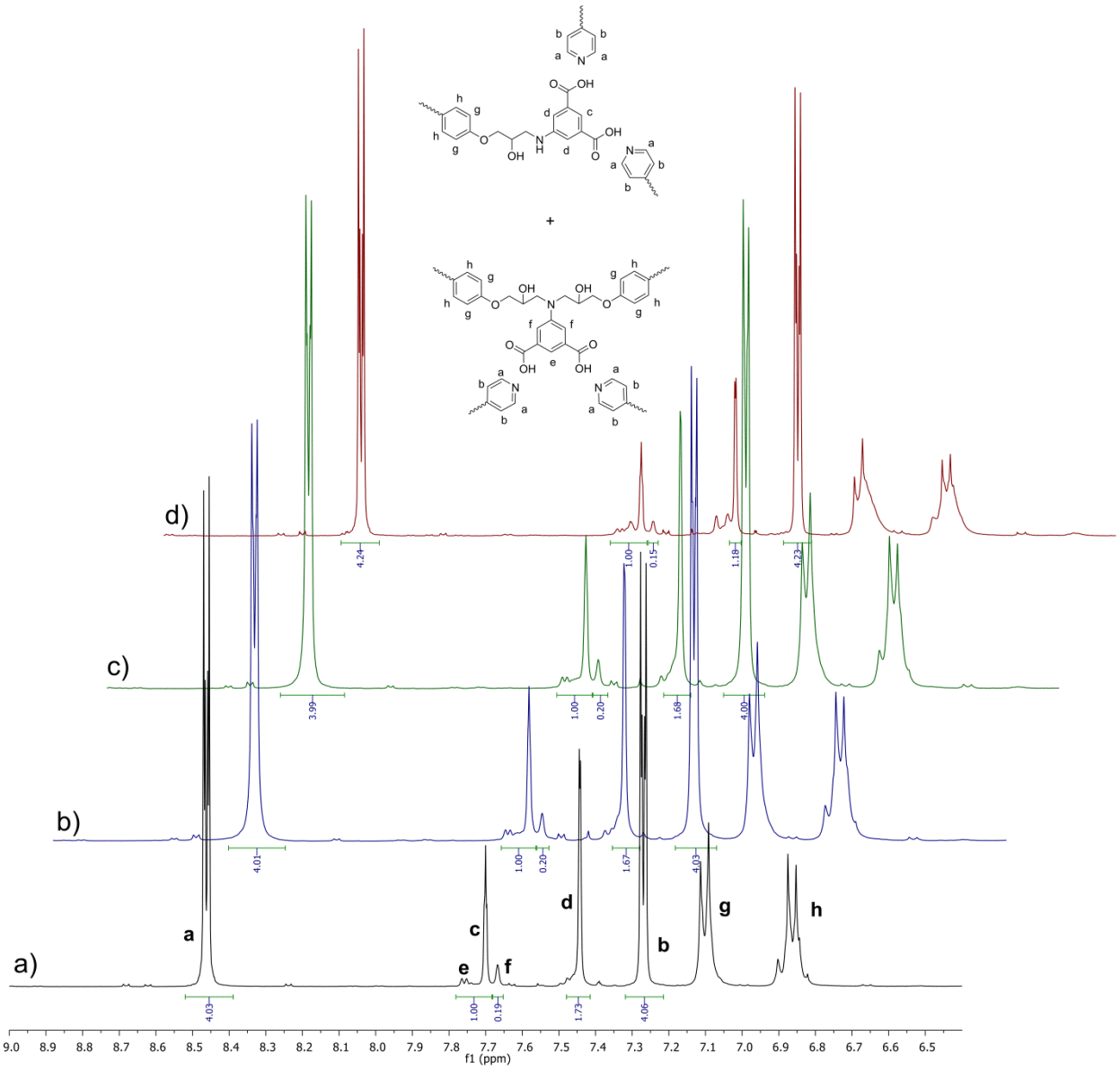

Figure S20. ^{1}H NMR spectra with assignments (only the region of the supramolecular cross-linking points are shown for the shake of clarity) of a) **P1b** (3-point bending sample), b) **P1b1**, c) **P1b2**, and c) **P1b** after 4h of shearing at 180 °C in the rheometer (see main text and Figure S14). In **P1b**, a 1:1 molar ratio between COOH (e.g. signals e+c) and pyridine (e.g. signal a) groups is observed. In the recycled samples **P1b1** and **P1b2**, the molar ratio is conserved. In d), the stoichiometry between pyridine and carboxylic acid units is lost and several other small signals appear.

9. Moisture uptake

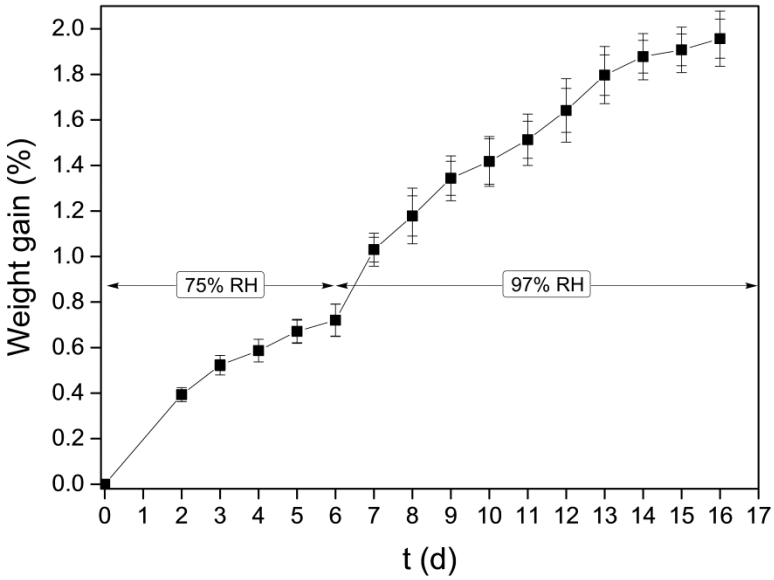

Figure S21. Moisture uptake of **P1b** as a function of time. The relative humidity was kept constant at 75% for 6 days and then it was increased to 97% for 10 additional days.

10. Single lap joint tests

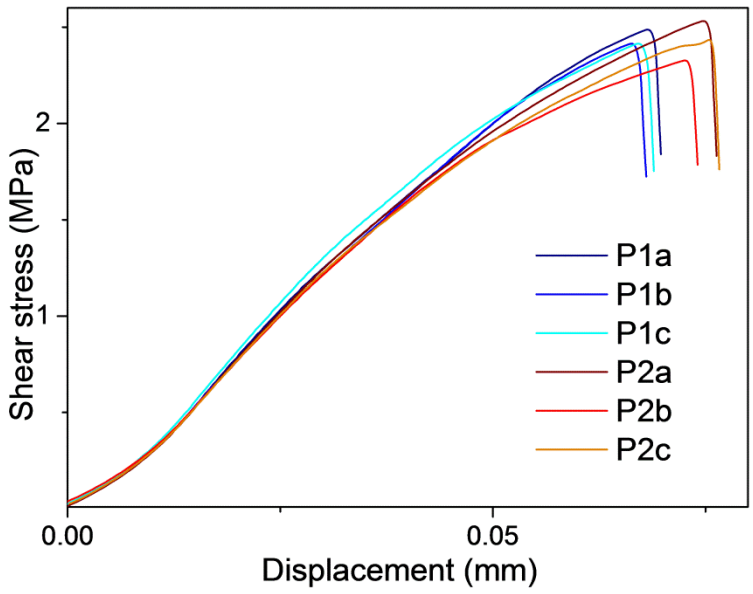

Figure S22. Shear stress vs. strain representative curves obtained on single lap joint tests with supramolecular networks **P1a-c and P2a-c**. Previously to each analysis, the lap joints were fixed with an initial clamping force of 1 N that was considered to determine the shear strength values displayed in Table 1 (the data for each polymer are average values of six independent tests).

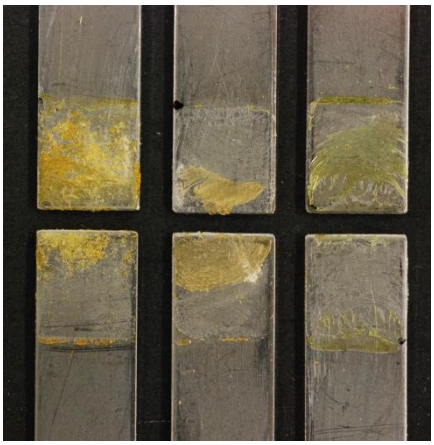

Figure S23. Pictures of representative lap joints of (from left to right) **P2a**, **P2b** and **P2c**, after failing upon mechanical testing.

11. Temperature profile under UV irradiation

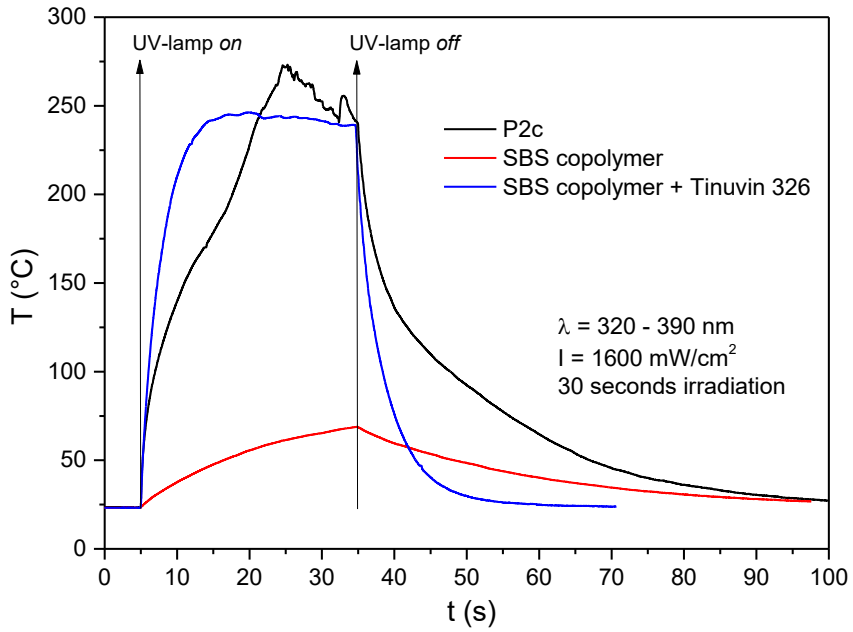

Figure S24. Temperature vs. time profiles of **P2c**, poly(styrene-b-butadiene-b-styrene) (M_n = 100,000 g/mol, 30 % styrene, SBS copolymer), and the same SBS copolymer blended with 0.25 wt% of Tinuvin 326 showing the effect of 30 seconds of UV-irradiation (λ = 320-390 nm, I = 1600 mW/cm^2).